

TABLE 1. OB Stars

Star	SpType	Ref <sup>a</sup>
HD 157955	B9 IV	1
HD 169033	B8 IV–Ve	1
HD 183143	B7 Ia	2
BD+24 3866	O8.5 Ib	3
HD 190429	O4 If <sup>+</sup>	4
HD 190603	B1.5 Ia <sup>+</sup>	5
HD 190864	O6.5 III(f)	6
HD 198183	B5/6 V	1
HD 198478	B2.5 Ia	5
HD 199579	O6 V((f))	4
HD 201254	B3 V	1

<sup>a</sup> SpType references: 1.) Bright Star Catalog, Hoffleit (1982) 2.) Morgan, Code, & Whitford (1955); 3.) Conti & Alschuler (1972); 4.) Walborn (1973); 5.) Lennon, Dufton, & Fitzsimmons (1992); 6.) Walborn (1972);

Notes to Table 1.

All spectra have a two pixel resolution of  $\lambda/\Delta\lambda \approx 570$ , except HD157955 and HD169033 which have  $\lambda/\Delta\lambda \approx 525$ ; see text.

TABLE 2. Hydrogen and Helium Equivalent Widths ( $\text{\AA}$ )

Line	$\lambda$ ( $\mu\text{m}$ )	HD190429	HD199579	HD190864	BD+24 3866	HD190603	HD198478	HD201254	HD198183	HD198183
Pa $\gamma$	1.0938	$2.0 \pm 0.2$	$3.9 \pm 0.5$	...	...	...	$4.7 \pm 0.2$	...	$7.1 \pm 0.2$	2
Pa $\beta$	1.2818	...	$5.6 \pm 0.7$	$4.0 \pm 1.0$	$4.4 \pm 1.0$	$4.8 \pm 0.7$	$6.0 \pm 0.8$	$8.5 \pm 0.8$	$9.1 \pm 0.8$	0
Br10	1.7362	...	...	...	...	$2.7 \pm 0.9$	$2.9 \pm 1.0$	$6.2 \pm 0.8$	$7.3 \pm 1.1$	2
He I	1.7002	$1.4 \pm 0.5$	$1.8 \pm 0.5$	$2.4 \pm 0.8$	$3.6 \pm 0.4$	$3.0 \pm 0.4$	$2.4 \pm 0.4$	$1.8 \pm 0.5$	$1.6 \pm 0.6$	1
Br11	1.6807	...	...	...	...	$3.4 \pm 0.9$	$3.3 \pm 1.0$	$6.3 \pm 0.8$	$7.7 \pm 1.1$	3
Br12	1.6407	...	...	...	...	$3.4 \pm 0.9$	$3.3 \pm 1.0$	$5.0 \pm 0.8$	$6.3 \pm 1.1$	2
Br13	1.6109	...	...	...	...	$3.0 \pm 0.9$	$2.7 \pm 1.0$	$4.1 \pm 0.8$	$4.5 \pm 1.1$	2
Br14	1.5880	...	...	...	...	$1.3 \pm 0.9$	$1.6 \pm 1.0$	$2.2 \pm 0.8$	$2.4 \pm 1.1$	1
Br15	1.5701	...	...	...	...	$1.8 \pm 0.9$	$2.2 \pm 1.0$	$2.1 \pm 0.8$	$2.1 \pm 1.1$	1
Br16	1.5557	...	...	...	...	$1.1 \pm 0.9$	$1.2 \pm 1.0$	$0.5 \pm 0.8$	$0.6 \pm 1.1$	1
Br17	1.5439	...	...	...	...	$0.4 \pm 0.9$	$1.3 \pm 1.0$	...	...	1
Br18	1.5342	...	...	...	...	$0.9 \pm 0.9$	$1.0 \pm 1.0$	...	...	1
Br19	1.5261	...	...	...	...	$0.8 \pm 0.9$	$0.8 \pm 1.0$	...	...	2
Br20	1.5192	...	...	...	...	...	...	...	...	1
Br21	1.5133	...	...	...	...	...	...	...	...	1

Notes to Table 2.

Hydrogen and Helium absorption strengths are in  $\text{\AA}$ . The line wavelengths are given in air (see text). Lines were measured by fitting the continuum and the line. The errors are the formal one sigma errors based on the rms scatter in the continuum and do not reflect the line fit.

# *H*–Band Spectroscopic Classification of OB Stars

R. D. Blum<sup>1</sup>, T. M. Ramond, P. S. Conti  
JILA, University of Colorado  
Campus Box 440, Boulder, CO, 80309  
rblum@casa.colorado.edu  
ramond@casa.colorado.edu  
pconti@jila.colorado.edu

D. F. Figer  
Division of Astronomy, Department of Physics & Astronomy,  
University of California, Los Angeles, CA, 90095  
figer@astro.ucla.edu

K. Sellgren  
Department of Astronomy, The Ohio State University  
174 W. 18th Ave., Columbus, OH, 43210  
sellgren@payne.mps.ohio-state.edu  
*accepted for publication in the AJ*

## ABSTRACT

We present a new spectroscopic classification for OB stars based on *H*–band (1.5  $\mu\text{m}$  to 1.8  $\mu\text{m}$ ) observations of a sample of stars with optical spectral types. Our initial sample of nine stars demonstrates that the combination of He I 1.7002  $\mu\text{m}$  and H Brackett series absorption can be used to determine spectral types for stars between  $\sim$  O4 and B7 (to within  $\sim \pm 2$  sub–types). We find that the Brackett series exhibits luminosity effects similar to the Balmer series for the B stars. This classification scheme will be useful in studies of optically obscured high mass star forming regions. In addition, we present spectra for the OB stars near 1.1  $\mu\text{m}$  and 1.3  $\mu\text{m}$  which may be of use in analyzing their atmospheres and winds.

*Subject headings:* infrared: stars — stars: early–type — stars: fundamental parameters

---

<sup>1</sup>Hubble Fellow

## 1. INTRODUCTION

OB stars are massive and thus short lived. Because they have short lives, they will be confined to regions relatively close to their birthplaces and will be found close to the Galactic plane. The youngest massive stars will also still be in or near their dusty star forming environment. Due to the strong extinction from interstellar dust at optical wavelengths, OB stars at large distances from the sun, or in young star forming regions, are more easily studied at near infrared ( $1 - 5 \mu\text{m}$ ) or longer wavelengths. Note that the extinction at  $V$  is about 10 times greater in *magnitudes* than at  $2.2 \mu\text{m}$ , and for  $\lesssim 3.5 \lambda \gtrsim 0.9 \mu\text{m}$ , the extinction can be represented by a power-law dependence:  $A_\lambda / A_{2.2\mu\text{m}} = (\lambda/2.2)^{-1.7}$  (Mathis 1990).

The advent of sensitive infrared array detectors has made near infrared classification schemes commonplace for a wide range of stellar spectral types. For example, Kleinmann & Hall (1986), Greene & Meyer (1995), Ali et al. (1995), and Ramírez et al. (1997) have presented  $K$ -band spectra of late-type stars useful for classification at  $2 \mu\text{m}$ . Lançon & Rocca-Volmerange (1992) have presented  $H$  and  $K$  spectra of optically classified stars ranging in spectral type from O6 to M7 (only three OB stars were included). Eenens et al. (1991), Blum et al. (1995a), Tamblyn et al. (1996), Morris et al. (1996), and Figer et al. (1996, 1997) have presented  $K$ -band spectra of known Wolf-Rayet and other emission-line stars. A detailed classification scheme in the  $K$ -band for early-type (OB) stars has been presented by Hanson & Conti (1994) and Hanson et al. (1996, hereafter HCR96). All these infrared classification spectra are now routinely applied to the study of obscured stars, typically in star forming regions and/or along sight lines with large interstellar obscuration by dust (e.g. Greene & Meyer 1995; Blum et al. 1995a,b; Tamblyn et al. 1996; Figer et al. 1996; Ali 1996; Blum et al. 1996).

Classification of hot stars at near infrared wavelengths is challenging because the photospheric absorption features used in the classification (primarily H, He I, and He II) are generally weaker than the molecular and atomic (metal) lines used for late-type stars. In addition, there can also be strong circumstellar emission which dilutes the photospheric lines. It is this latter problem that motivates the present work. Since we expect circumstellar dust emission to dominate the  $K$ -band spectra of some stars in star forming regions (e.g., in M17, Hanson & Conti 1995), a more robust classification scheme for high mass star forming regions will also utilize shorter wavelengths which may be less affected by circumstellar excess emission. Conversely, we wish to observe at the longest possible wavelengths shortward of  $K$  to overcome the extinction of intervening dust. In this paper, we present a preliminary classification of OB stars based on spectra between  $1.5 \mu\text{m}$  and  $1.8 \mu\text{m}$  (i.e. in the  $H$ -band). We also present spectra of the same stars between  $1 \mu\text{m}$

and  $1.3 \mu\text{m}$  which may prove useful in the analysis of massive stars atmospheres.

## 2. OBSERVATIONS and DATA REDUCTION

The OB stars were observed on the nights of 9, 10, and 13 June 1996 using the Ohio State Infrared Imager and Spectrometer (OSIRIS) on the Perkins 1.8-m telescope of the Ohio Wesleyan and Ohio State Universities at the Lowell Observatory. The Perkins telescope is located on Anderson Mesa near Flagstaff, Arizona. OSIRIS is more fully described by DePoy et al. (1993). The target stars were taken from the catalog of HCR96 and are listed, along with their optical spectral types, in Table 1. In addition to the target OB stars, we observed A-type and G-type stars for use in canceling telluric absorption features. We will refer to these stars as “atmospheric standards.”

OSIRIS was used in cross-dispersed mode which gives  $\lambda/\Delta\lambda \approx 570$  (2 pixels) while covering the  $J$  ( $\lambda_o \approx 1.25 \mu\text{m}$ ,  $\Delta\lambda \approx 0.30 \mu\text{m}$ ),  $H$  ( $\lambda_o \approx 1.65 \mu\text{m}$ ,  $\Delta\lambda \approx 0.37 \mu\text{m}$ ), and  $K$  ( $\lambda_o \approx 2.20 \mu\text{m}$ ,  $\Delta\lambda \approx 0.50 \mu\text{m}$ ) bands simultaneously. One star (HD183143) was also observed in long slit mode at  $J$  and  $H$ . Long slit mode is similar to the cross-dispersed mode (same spectral resolution and spatial scale) except only one wavelength band is acquired at a time and the long slit fills the entire spatial dimension on the array. Similar results were obtained from both sets of spectra; however, the long slit mode spectra are slightly higher S/N and are therefore presented here. In addition, five of the stars observed in cross-dispersed mode were also observed at  $\lambda \approx 1.10 \mu\text{m}$  ( $\Delta\lambda \approx 0.25 \mu\text{m}$ ), a bandpass which we call  $I'$ , in long slit mode. Analysis of  $H$ -band OH sky lines results in linear dispersions of 9.70, 11.60, 14.53, and 19.37  $\text{\AA} \text{ pix}^{-1}$  at  $I'$ ,  $J$ ,  $H$ , and  $K$ , respectively. The sky lines were identified using the list of Oliva & Origlia (1992).  $I'$ ,  $J$ , and  $K$  band dispersions follow from the  $H$ -band dispersion and the appropriate order number,  $m$  ( $m = 6, 5, 4, 3$  for  $I'$ ,  $J$ ,  $H$ ,  $K$ ). In cross-dispersed mode, OSIRIS has a  $\sim 60'' \times 5''$  slit ( $1.5'' \text{ pix}^{-1}$ ). The target stars were observed at  $\gtrsim 12$  uniformly spaced positions along the slit. Combining spectra over a uniform grid along the slit greatly reduces systematic errors which may be introduced, for example, by scattered light in the dome flats and fringing (see Blum et al. 1995a for a discussion of these problems in OSIRIS). The seeing varied throughout each night from  $2''$  to  $4''$ . None of the nights were photometric; we observed through thin clouds. This will not affect our results since we are interested in the relative intensities and line strengths, not absolute fluxes.

All basic data reduction was accomplished using IRAF<sup>2</sup>. Each image was flat–fielded using dome flats and then sky subtracted using another image from the grid with the star displaced by several positions along the slit (cross–dispersed mode) or with a median combination sky image (long slit mode). Individual spectra were extracted from each program star image and atmospheric standard image using IRAF “APEXTRACT.” Synthesized apertures  $\pm 3$  pixels wide were used. The entire grid of 1–d spectra for each star was then combined (after scaling). In the case of the long slit spectra, the individual 1–d spectra were first shifted (0 to  $\sim 4$  pixels) to account for anamorphic demagnification along the slit spatial dimension.

The final spectra were obtained by ratioing the program stars with a atmospheric standard star which had first been corrected for intrinsic H absorption lines ( $P\beta$  1.281  $\mu\text{m}$ , and Brackett series 1.51  $\mu\text{m}$  to 2.165  $\mu\text{m}$ ). The atmospheric standards were observed in pairs of A–type and G–type stars. The H lines in the A stars were corrected in the following way. The majority (seven) of our program stars were corrected using an A0 V and a G2 V. In this case, the G2 star (BS 6847) was first corrected for H line absorption using the NOAO solar atlas (Livingston & Wallace 1991). Next a ratio of the A star (BS 7734) to the corrected G star was made. Since these two were taken at nearly the same airmass, the resulting ratio contains essentially only the H line spectrum of the A star and perhaps some “emission” lines due to metal lines in the G star. The H lines in this ratio were then fit with Gaussian profiles. The resultant line fits were used to correct the H absorption in the A star. The two remaining stars (HD183143 and BD+24 3866) were corrected using an A3 V (BS 7958) and a G9 III (BS 7760). We have no intrinsic spectrum to correct BS 7760 with, so the  $J$  and  $K$ –band lines were corrected by eye. No correction was made for the  $H$ –band Brackett lines in BS 7760. Since BS 7760 was not corrected using a matching intrinsic H spectrum, we are less confident in the precise H line absorption resulting in HD183143 and BD+24 3866; however, none of our primary results is sensitive to the accuracy of our measurement of H absorption in the program stars but only the appearance or absence of a definitive Brackett series. No telluric correction was made for the  $I'$  spectra as a cursory inspection of the spectra shows no strong telluric lines. We did obtain A and G star spectra for use in making a similar telluric correction as described above. Making this correction shows no difference in the final  $I'$  spectra of the OB stars at the few percent level and serves only to introduce more noise.

We have also included two  $H$ –band spectra (HD 157955 and HD 169033) which were

---

<sup>2</sup>IRAF is distributed by the National Optical Astronomy Observatories.

obtained as part of a program concentrating on  $K$ –band spectra of stars in an inner Galaxy star forming region called the Quintuplet (Figer et al. 1996). These spectra have similar spectral ( $16.75 \text{ \AA pix}^{-1}$ ) resolution as the OSIRIS data and spatial scale somewhat smaller ( $0.7'' \text{ pix}^{-1}$ ); see Figer et al. (1995). The telluric correction was made by ratioing the stars to a Quintuplet star (q3 in Moneti et al. 1994) and a dusty Wolf-Rayet star (WR118), neither of which have spectral lines near the He I or Brackett lines. These stars were observed at higher airmass ( $\sim 2$ ) than the other stars presented here ( $\sim 1$ ) and may not be corrected as well (the higher Brackett lines appear to suffer from incomplete correction).

### 3. RESULTS and DISCUSSION

#### 3.1. The $H$ –band Spectra

The final  $H$ –band spectra are shown in Figure 1. To highlight the absorption features, we have divided each spectrum by a low order fit to the continuum. We do not present our  $K$ –band spectra here since spectra for these stars have been presented by HCR96 (at higher spectral resolution). We note that our lower resolution  $K$ –band spectra reproduce the basic features of the HCR96 spectra. Line identifications used throughout this paper were taken from Weise et al. (1966, H, He I), and Garcia & Mack (1965, He II). All wavelengths used and/or quoted are in air. Line equivalent widths (Table 2) were measured by fitting Gaussian profiles using the LINER program (Pogge 1997). Uncertainties are the formal one sigma errors derived from the rms scatter in the continuum corresponding to a bandpass equal to the full width at zero intensity of the lines. The errors do not reflect the line fit.

##### 3.1.1. The Brackett Series

The H lines are sensitive to the excitation in the stellar atmosphere. For example, the strength of the well-known Balmer lines increases with  $T_{\text{eff}}$  as more atoms are excited to the  $n=2$  level. The Balmer lines reach peak strength at  $\sim 9000 \text{ K}$  (Gray 1992) as Hydrogen becomes appreciably ionized at higher temperatures. The Brackett series excitation is similar to that for the Balmer series (10.8 eV compared to 10.2 eV), so we expect the lines to behave in a similar manner. This basic behavior with  $T_{\text{eff}}$  (spectral type) is seen in Figure 1.

Inspection of Figure 1 suggests the Brackett lines behave similarly to the Balmer lines in early-type stars as first noted by Adams & Joy (1922, 1923): the width of the H lines decreases with stellar luminosity for the B stars; further, the last line visible in the series

increases with luminosity. Br19 is confidently detected in the B supergiants while Br15 or Br16 is the last of the series for the B dwarfs. The measured line widths (FWHM  $\sim 60 \text{ \AA}$  for Br11–Br15) for the two B dwarf stars are roughly two times the instrumental resolution (FWHM =  $29 \text{ \AA}$ ). This can be compared to a maximum of  $44 \text{ \AA}$  in the B supergiants for the same lines. These “luminosity” effects are well understood as resulting from the linear Stark effect (Hulbert 1924; Struve 1929; Gray 1992) which is sensitive to the electron pressure.

In Figure 1 it can be noted that the upper Brackett lines are missing in the earliest O-type stars, although Br $\gamma$  is present in these same stars (HCR96). There are, as yet, no published model predictions for the upper Brackett series lines, but we suspect their absence in the earliest O-type stars, while Br $\gamma$  is still present, is analogous to the case for the Balmer lines. LTE model predictions of Auer & Mihalas (1972) clearly underestimate H $\gamma$  absorption compared to observations, while their non-LTE predictions provide a much better fit (Conti 1973). Peterson & Scholz (1971) demonstrate that the difference between the observations and LTE predictions is much less for the higher series member H8 than for H $\gamma$ . The upper series members of the Brackett lines probably are still close to LTE (similar to H8) and thus, quite weak due to the advanced ionization state of hydrogen. The lower series members, such as Br $\gamma$ , exhibit non-LTE behavior (similar to H $\gamma$ ) and are thus still present.

### 3.1.2. He I and He II

A relatively strong line of He I (4–3) is visible at  $1.7002 \mu\text{m}$ . To be useful for classification purposes, the wavelength range of interest must contain various lines sensitive to different excitation in the stellar atmosphere. In the present case, the Brackett series lines (as discussed above) and He I  $1.7002 \mu\text{m}$  line are sensitive to lower and higher  $T_{\text{eff}}$ , respectively, in the atmospheres of OB stars. In Figure 2, we plot the equivalent width of the He I (4–3)  $1.7002 \mu\text{m}$  line versus the spectral type (Table 1). This line is at maximum strength in the late O/early B types. In the earliest O stars, the Brackett series will be weak or absent (Figure 1), whereas in the late B stars, the Brackett lines are stronger. These features, therefore, provide a rough spectral class in the  $H$ –band for stars in the range  $\sim$  O4 to B7 (Figure 2 suggests a spectral type could be determined to  $\sim \pm 2$  sub-types). Note that He I  $1.7002 \mu\text{m}$  is detected in HD183143 (B7 Ia) even though the telluric correction appears worse for this star: compare the region just to the red wavelength side of the  $1.7 \mu\text{m}$  line. The dip in the spectrum is due to a relatively poor air–mass match between object and standard, but the He I  $1.7002 \mu\text{m}$  line is visible in the uncorrected spectrum.

Figure 3 shows a more detailed look at the  $H$ –band spectra of the four O stars. The



figure suggests a tentative detection of He II (13-7) at  $1.5719 \mu\text{m}$  and perhaps He II (12-7) at  $1.6918 \mu\text{m}$ . The former is clearly in a region of higher signal-to-noise; the latter sits in a region with larger telluric features (the strongest of which are to the blue of the He I  $1.7002 \mu\text{m}$  line). The  $1.5719 \mu\text{m}$  line appears in both of the O star spectra of Lançon & Rocca-Volmerange (1992) as well, including their spectrum of HD 199579, one of the stars observed in our sample. Detection of He II is difficult since the  $1.5719 \mu\text{m}$  line is near the Brackett 15-4 line ( $1.5701 \mu\text{m}$ ); and hence, the He II line could depend on how well we have corrected the Brackett series lines in the A star which was used as an atmospheric standard (see §2). The He II lines may prove more useful when observed at higher spectral resolution.

### 3.2. $I'$ and $J$ -band Spectra

Figure 4 shows spectra of the OB stars near  $1.1$  and  $1.3 \mu\text{m}$ . The primary lines which fall within our  $I'$  and  $J$ -band spectra are due to H and He I, as in the  $H$ -band spectra. However the H lines,  $\text{Pa}\gamma$  ( $1.0938 \mu\text{m}$ ) and  $\text{Pa}\beta$  ( $1.2818 \mu\text{m}$ ) are blended with lines of He I and He II at our resolution (see Figure 4), so they are of limited use for determining spectral types. We note that He I  $1.0830 \mu\text{m}$  is present in several of the stars (HD190429, P Cygni profile; HD183143). We anticipate that the behavior of this triplet line ( $2p^3P^\circ-2s^3S$ ) will *not* be well correlated with spectral type, following the example of the analogous singlet He I feature at  $2.0581 \mu\text{m}$  (HCR96). We have only five  $I'$  spectra in our initial sample, so we do not attempt to make any firm conclusions about this wavelength region. In any case, the  $I'$  and  $J$ -bands should be useful for comparison to model atmosphere predictions, especially when they are obtained for “free,” i.e. in cross-dispersed mode.

## 4. SUMMARY

We have presented  $H$ -band spectra of a preliminary set of OB stars and identified absorption features that can be used to classify young, massive stars in obscured H II regions and/or along sight lines with large optical extinction due to interstellar dust. The absorption strength of the He I (4-3)  $1.7002 \mu\text{m}$  line, in conjunction with the presence or absence of the  $H$ -band lines of the Brackett series, is well correlated with optical spectral types and can be used as a coarse spectral classification. The behavior of the infrared lines is analogous to well-studied lines in the optical wavelength region including basic effects due to excitation (temperature) and gravity (pressure). In particular, we see the effects of linear Stark broadening, resulting from changes in pressure in B dwarfs and supergiants, on the Brackett lines which will be useful as a luminosity indicator in the B stars. We

have also presented spectra of the OB stars between 1.1 and 1.3  $\mu\text{m}$ . Features in these wavelength regions may prove useful in cases where excess emission is still strong at  $H$  or for the purposes of testing atmosphere models of hot stars.

Support for this work was provided by NASA through grant number HF 01067.01 – 94A from the Space Telescope Science Institute, which is operated by the Association of Universities for Research in Astronomy, Inc., under NASA contract NAS5–26555. OSIRIS was built with support from NSF grants AST 90–16112 and AST 9218449. This work was also supported by NSF grant AST 93–14808.

## REFERENCES

- Adams, W. S. & Joy, A. H. 1922, *ApJ*, 56, 242
- Adams, W. S. & Joy, A. H. 1923, *ApJ*, 57, 294
- Ali, B., Carr, J. S., DePoy, D. L., Frogel, J. A., & Sellgren, K. 1995, *AJ*, 110, 2415
- Ali, B. 1996, PhD Dissertation, The Ohio State University, Columbus, OH.
- Auer, L. & Mihalas, D. 1972, *ApJS*, 24, 193
- Blum, R. D., DePoy, D. L., & Sellgren, K. 1995*a*, *ApJ*, 441, 603
- Blum, R. D., Sellgren, K., & DePoy, D. L. 1995*b*, *ApJ*, 440, L17
- Blum, R. D., Sellgren, K., & DePoy, D. L. 1996, *AJ*, 112, 1988
- Conti, P. S. 1973, *ApJ*, 179, 161
- DePoy, D. L., Atwood, B., Byard, P., Frogel, J. A., & O’Brien, T. 1993, in *SPIE 1946*, “Infrared Detectors and Instrumentation,” pg 667
- Eenens, P. R. J., Williams, P. M., & Wade, R. 1991, *MNRAS*, 252, 300
- Figer, D. F., Morris, M., & McLean, I. S. 1995, *ApJ*, 447, L29
- Figer, D. F., Morris, M., & McLean, I. S. 1996, in *The Galactic Center 4th ESO/CTIO Workshop*, Ed. R. Gredel, *PASP Conf. Ser.*, Vol. 102, p 263
- Figer, D. F., McLean, I. S., & Najarro, F. 1997, *ApJS*, submitted
- Garcia, J. D. & Mack, J. E. 1965, *J. Opt. Soc. Am.*, 55, 654
- Gray, D. F. 1992, *The Observation and Analysis of Stellar Photospheres*, Cambridge University Press, Cambridge, p219–225, 291
- Greene, T. P. & Meyer, M. R. 1995, *ApJ*, 450, 233
- Hanson, M. M. & Conti, P. S. 1994, *ApJ*, 423, L129
- Hanson, M. M. & Conti, P. S. 1995, *ApJ*, 448, L45
- Hanson, M. M., Conti, P. S., & Rieke, M. J. 1996, *ApJS*, 107 281 (HCR96)
- Hoffleit, D., 1982, *The Bright Star Catalog*, Yale University Press, New Haven
- Hulburt, E. O. 1924, *ApJ*, 59, 177
- Kleinmann, S.G. & Hall, D.N.B. 1986, *ApJS*, 62, 501
- Lançon, A. & Rocca-Volmerange, B. 1992, *A&AS*, 96, 593
- Lennon, D. J., Dufton, P. L., & Fitzsimmons, A. 1992, *A&AS*, 94, 569
- Livingston, W. & Wallace, L. 1991, *N.S.O. Technical Report #91–001*, 1991 July

- Mathis, J.S. 1990, *ARA&A*, 28, 37
- Moneti, A., Glass, I. S., & Moorwood, A. F. M. 1994, *MNRAS*, 268, 194
- Morris, P. M., Hanson, M. M., Conti, P. S., Eenens, P. R. J., & Blum, R. D. 1996, *ApJ*, 470, 597
- Oliva, E. & Origlia, L. 1992, *A&A*, 254, 466
- Peterson, D. M. & Scholz, M. 1971, *ApJ*, 163, 51
- Pogge, R. 1997, private communication
- Ramírez, S. V., DePoy, D. L., Frogel, J. A., Sellgren, K., & Blum, R. D. 1997, *AJ*, in press
- Struve, O. 1929, *ApJ*, 69, 173
- Tamblyn, P., Rieke, G. H., Hanson, M. M., Close, L. M., McCarthy, D. W., JR., & Rieke, M. J. 1996, *ApJ*, 456, 206
- Wiese, W. L., Smith, M. W., Glennon, B. M. 1966, *Atomic Transition Probabilities*, United States Dept. of Commerce, report no. NSRDS–NBS 4

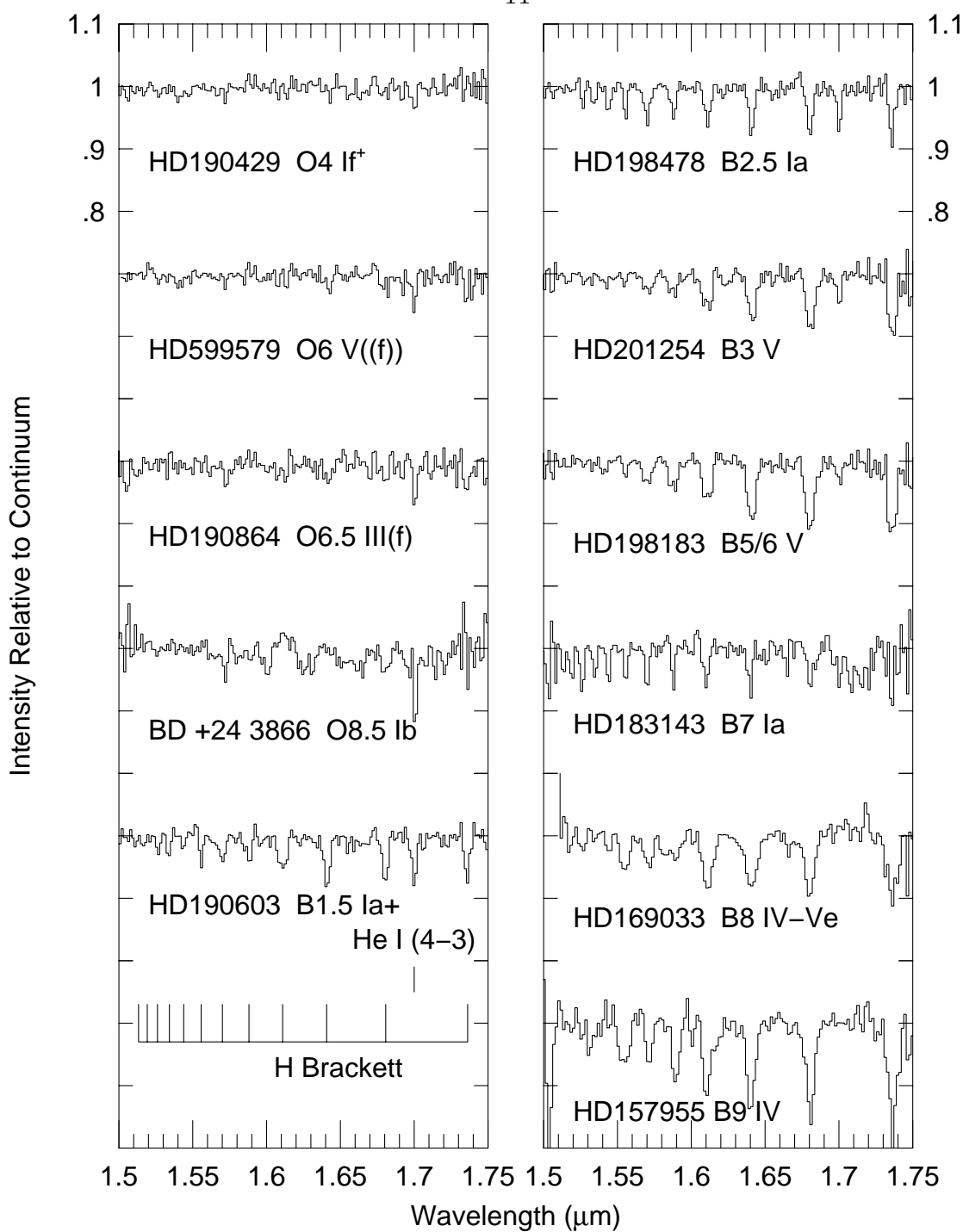


Fig. 1.—  $\lambda/\Delta\lambda \approx 570$   $H$ -band spectra of OB stars (The two latest B stars are from an independent data set and have  $\lambda/\Delta\lambda \approx 525$ ; see text). The spectra have been normalized by a low order fit to the continuum. He I  $1.7002 \mu\text{m}$  and H Brackett lines are the key to the present  $H$ -band classification of OB stars. The first Brackett line is Br10. See text and Figure 2. The intensity scale is the same for each star.

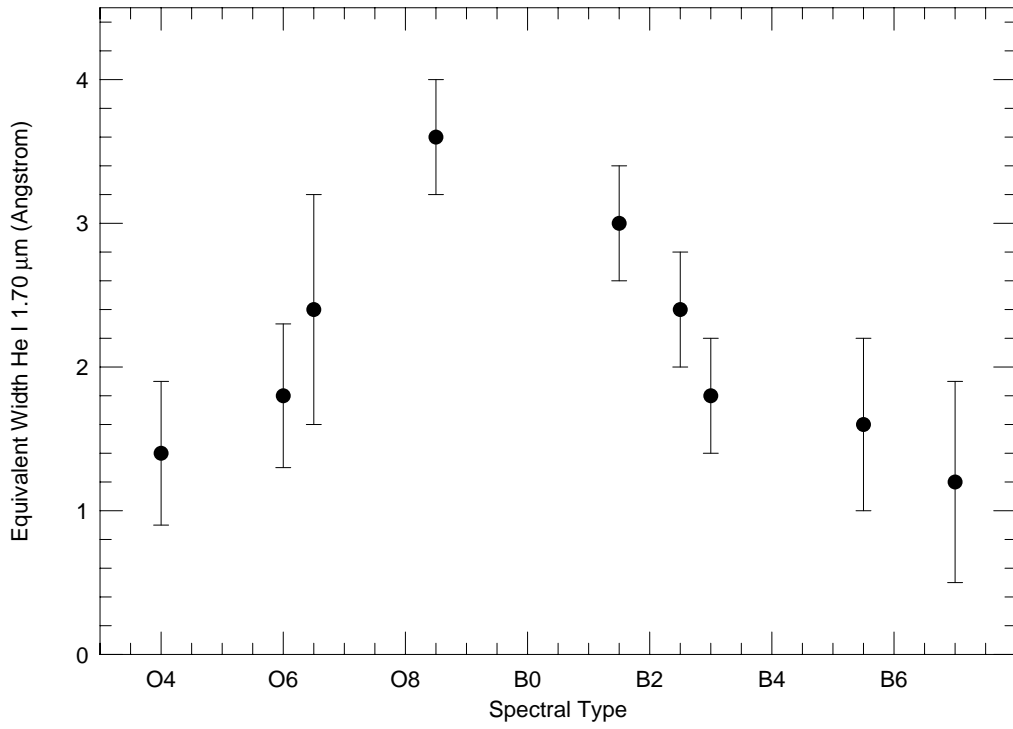


Fig. 2.— He I 1.7002  $\mu\text{m}$  equivalent width versus spectral type. O type stars and late B type stars are distinguished by the presence or absence of H Brackett absorption; see Figure 1.

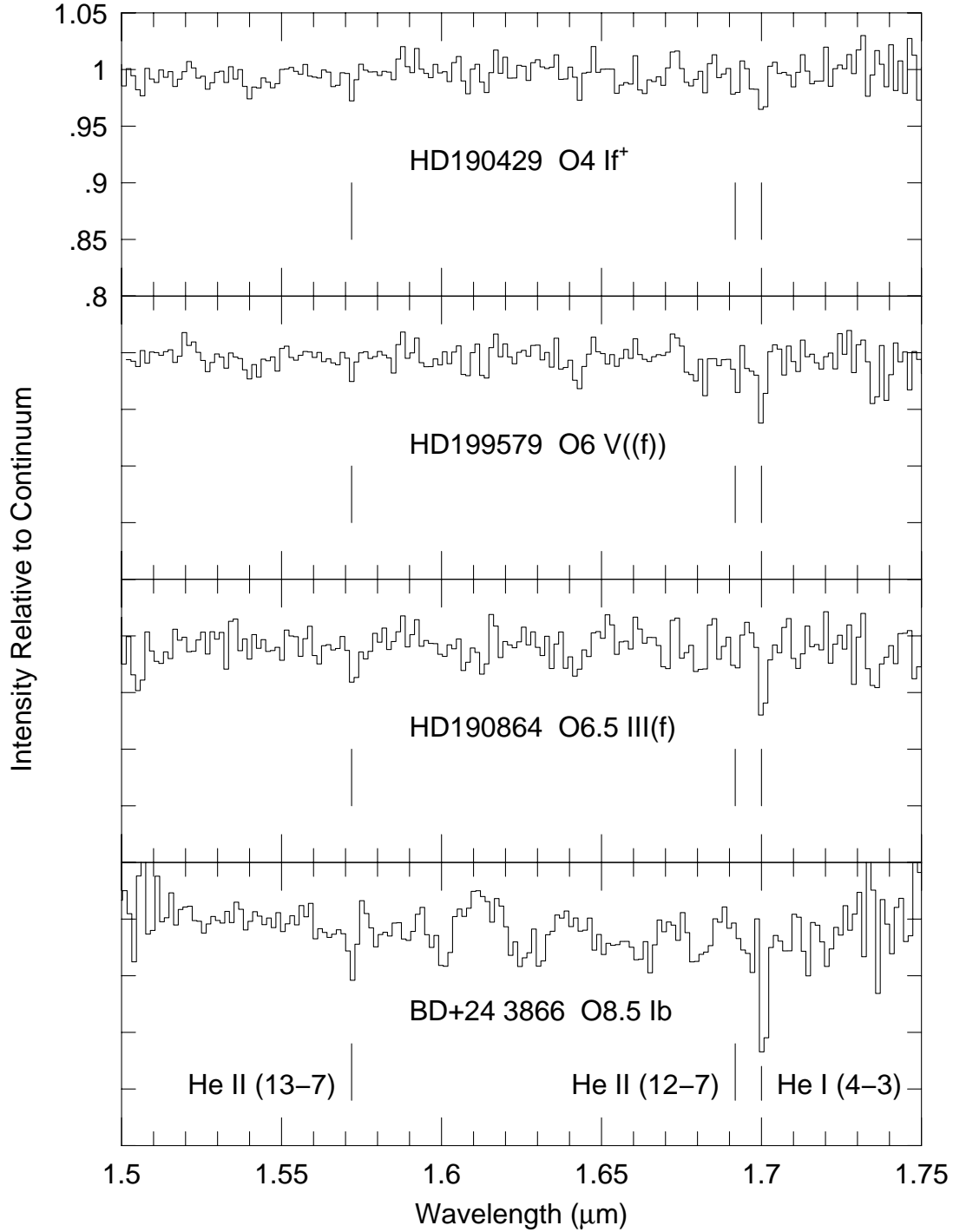


Fig. 3.— Detail of  $H$ -band spectra for the O stars (same spectra as plotted in Figure 1) showing probable He II absorption at  $1.5719 \mu\text{m}$ . He II  $1.6918 \mu\text{m}$  absorption is marked although not clearly detected; see text. The intensity scale is the same for each star.

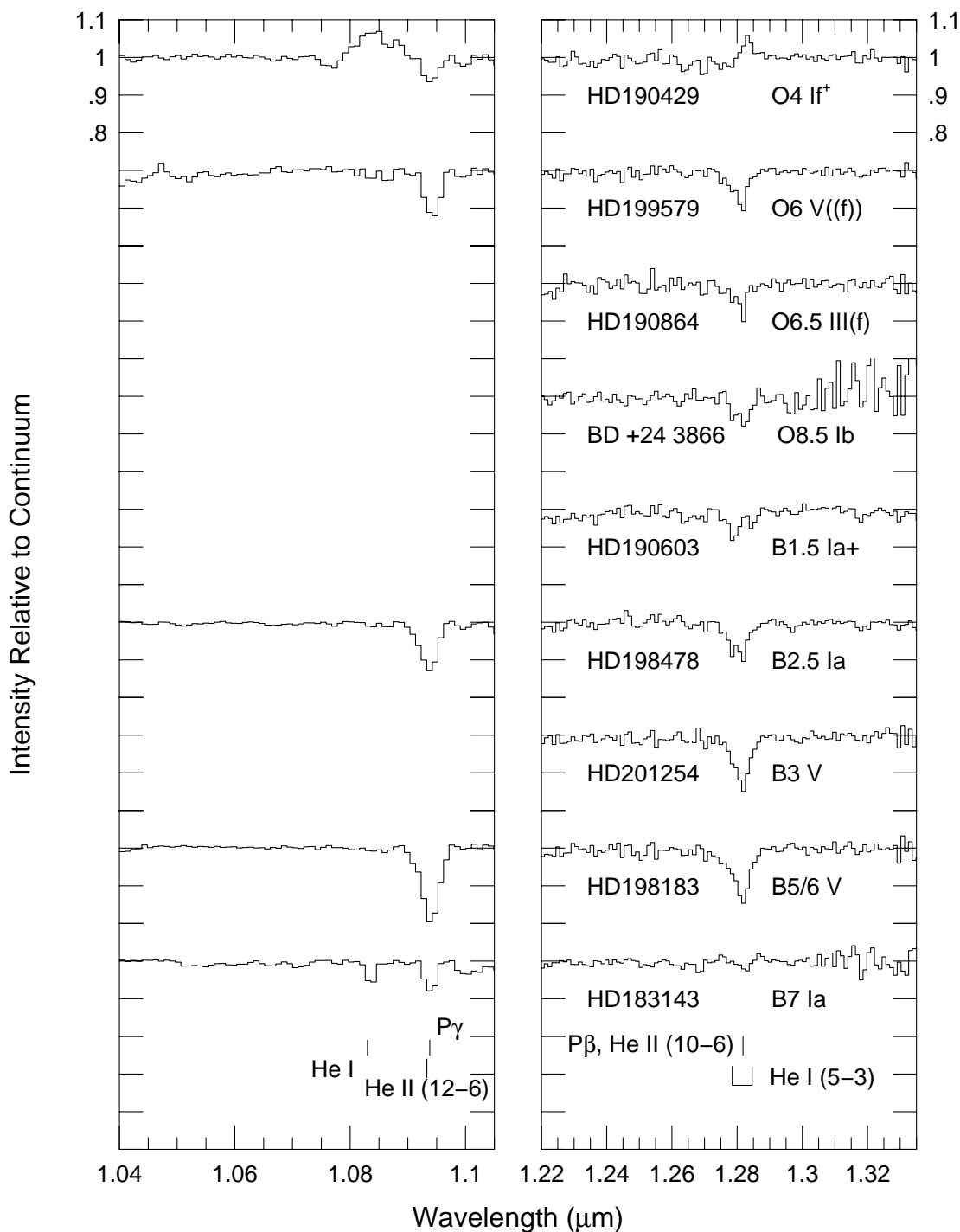


Fig. 4.—  $\lambda/\Delta\lambda \approx 570$   $I'$  and  $J$ -band spectra of OB stars. The spectra have been normalized by a low order fit to the continuum. Pa $\gamma$  (1.0938  $\mu\text{m}$ ) and Pa $\beta$  (1.2818  $\mu\text{m}$ ) may have contributions due to He I and He II. The intensity scale is the same for each star.